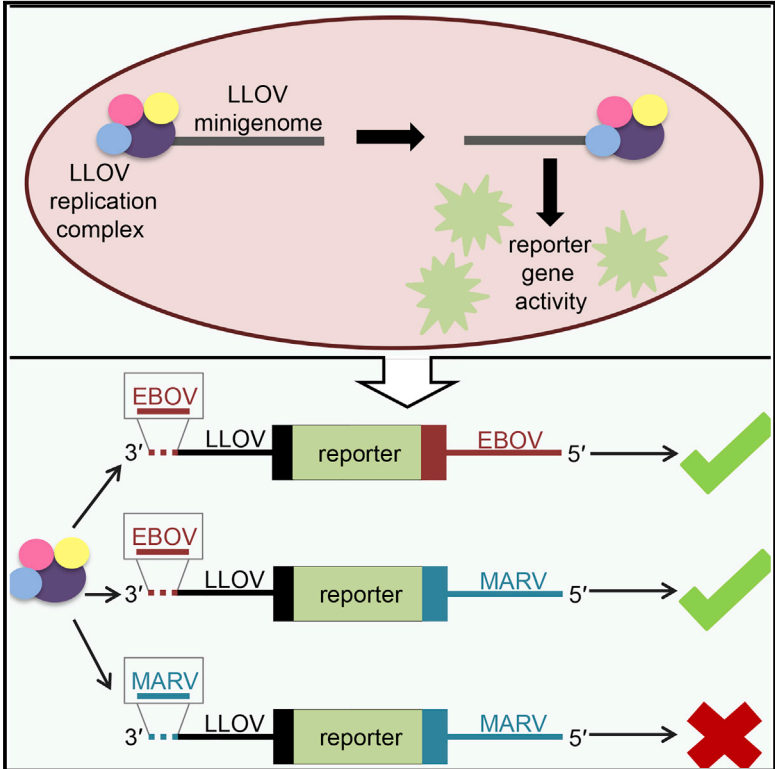


# Cell Reports

## A Chimeric Lloviu Virus Minigenome System Reveals that the Bat-Derived Filovirus Replicates More Similarly to Ebolaviruses than Marburgviruses

### Graphical Abstract



### Authors

Whitney A. Manhart, Jennifer R. Pacheco, Adam J. Hume, Tessa N. Cressey, Laure R. Deflubé, Elke Mühlberger

### Correspondence

muehlber@bu.edu

### In Brief

Lloviu virus (LLOV) is a filovirus of unknown pathogenicity, and the viral genome ends have not been recovered. Manhart et al. established a minigenome system for studying LLOV by complementing missing sequence information with that of other filoviruses. This minigenome provides a blueprint for generating recombinant LLOV for pathogenesis studies.

### Highlights

- The LLOV replication complex supports replication of chimeric LLOV minigenomes
- LLOV utilizes an ebolavirus-like replication strategy
- LLOV does not recognize the marburgvirus leader sequence
- The terminal genomic 3' nucleotides determine the specificity of the LLOV polymerase



# A Chimeric Lloviu Virus Minigenome System Reveals that the Bat-Derived Filovirus Replicates More Similarly to Ebolaviruses than Marburgviruses

Whitney A. Manhart,<sup>1,2,3</sup> Jennifer R. Pacheco,<sup>1,2,3</sup> Adam J. Hume,<sup>1,2</sup> Tessa N. Cressey,<sup>1,2</sup> Laure R. Deflubé,<sup>1,2</sup> and Elke Mühlberger<sup>1,2,4,\*</sup>

<sup>1</sup>Department of Microbiology, Boston University School of Medicine, Boston, MA 02118, USA

<sup>2</sup>National Emerging Infectious Diseases Laboratories, Boston University School of Medicine, Boston, MA 02118, USA

<sup>3</sup>These authors contributed equally

<sup>4</sup>Lead Contact

\*Correspondence: [muehlber@bu.edu](mailto:muehlber@bu.edu)

<https://doi.org/10.1016/j.celrep.2018.08.008>

## SUMMARY

Recently, traces of zoonotic viruses have been discovered in bats and other species around the world, but despite repeated attempts, full viral genomes have not been rescued. The absence of critical genetic sequences from these viruses and the difficulties to isolate infectious virus from specimens prevent research on their pathogenic potential for humans. One example of these zoonotic pathogens is Lloviu virus (LLOV), a filovirus that is closely related to Ebola virus. Here, we established LLOV minigenome systems based on sequence complementation from other filoviruses. Our results show that the LLOV replication and transcription mechanisms are, in general, more similar to ebolaviruses than to marburgviruses. We also show that a single nucleotide at the 3' genome end determines species specificity of the LLOV polymerase. The data obtained here will be instrumental for the rescue of infectious LLOV clones for pathogenesis studies.

## INTRODUCTION

The filovirus family contains three genera—*Ebolavirus*, *Marburgvirus*, and *Cuevavirus*. Many filoviruses, including Ebola virus (EBOV) and Marburg virus (MARV), cause a severe disease in humans with high case fatality rates. In contrast, Reston virus (RESTV), which belongs to the *Ebolavirus* genus, has not yet been associated with disease in humans, suggesting that RESTV may not be pathogenic for humans (Miranda and Miranda, 2011). Filovirus epidemics occur sporadically and are difficult to predict. A prime example is the 2013–2016 EBOV outbreak in West Africa that claimed at least 11,000 lives and resulted in billions of dollars of economic loss (Bausch, 2017). Epidemiological data suggest that a single spill-over event from an animal reservoir started this outbreak (Baize et al., 2014). Bats have been discussed as potential reservoir hosts for the West African EBOV variant (Marí Saéz et al., 2015), although isolation of infectious EBOV from any bat species has not yet been described. This is

different for the closely related MARV, for which Egyptian fruit bats (*Rousettus aegyptiacus*) have been identified as likely reservoir hosts (Towner et al., 2009). Egyptian rousettes are susceptible to experimental infection with both MARV and EBOV without developing symptoms of disease (Jones et al., 2015; Paweska et al., 2016).

Bats also played a role in the discovery of the most recent member of the filovirus family. This novel filovirus was discovered in the Cueva del Lloviu cave, Asturias, Spain, which is inhabited by *Miniopterus schreibersii* bats (Negredo et al., 2011). Viral RNA was isolated from bat carcasses, and using deep sequencing and PCR techniques, a nearly complete viral genomic sequence was compiled. At the sequence level, the new filovirus was clearly distinct from the known ebola- and marburgviruses and therefore was classified as a member of a new species, Lloviu virus (LLOV) within the new genus *Cuevavirus* (Amarasinghe et al., 2018). Recently, LLOV re-emerged in Northeast Hungary, and again, its emergence correlated with unexplained increased mortality among *Miniopterus schreibersii* bats (Kemenesi et al., 2018). The bats showed symptoms of respiratory bleeding, but it remains to be determined whether LLOV is the causative agent of the disease. Similar to the previous LLOV outbreak in Spain, it has not been possible to isolate infectious virus from the bat carcasses collected in Hungary. The lack of infectious LLOV significantly hampers research efforts aimed to study the pathogenic potential of this virus.

It is not known whether LLOV poses a health risk for the human population, yet the similarities to EBOV and MARV indicate that it could be pathogenic for humans. However, as mentioned above, the filoviruses considerably vary in terms of pathogenicity, and more research on LLOV biology is required to understand where it fits within the filovirus family. The genomic structure of LLOV is similar to that of other filoviruses (Figure 1A). The nonsegmented negative sense RNA genome is flanked by the 3' leader and the 5' trailer. These regions contain the replication and transcription promoters. The LLOV genome encodes the seven characteristic filoviral proteins: the nucleoprotein (NP); polymerase co-factor (VP35); matrix protein (VP40); glycoprotein (GP); transcription factor (VP30); nucleocapsid maturation protein (VP24); and RNA-dependent RNA polymerase (L). These proteins are homologous to those in other filovirus genomes (Negredo et al., 2011).



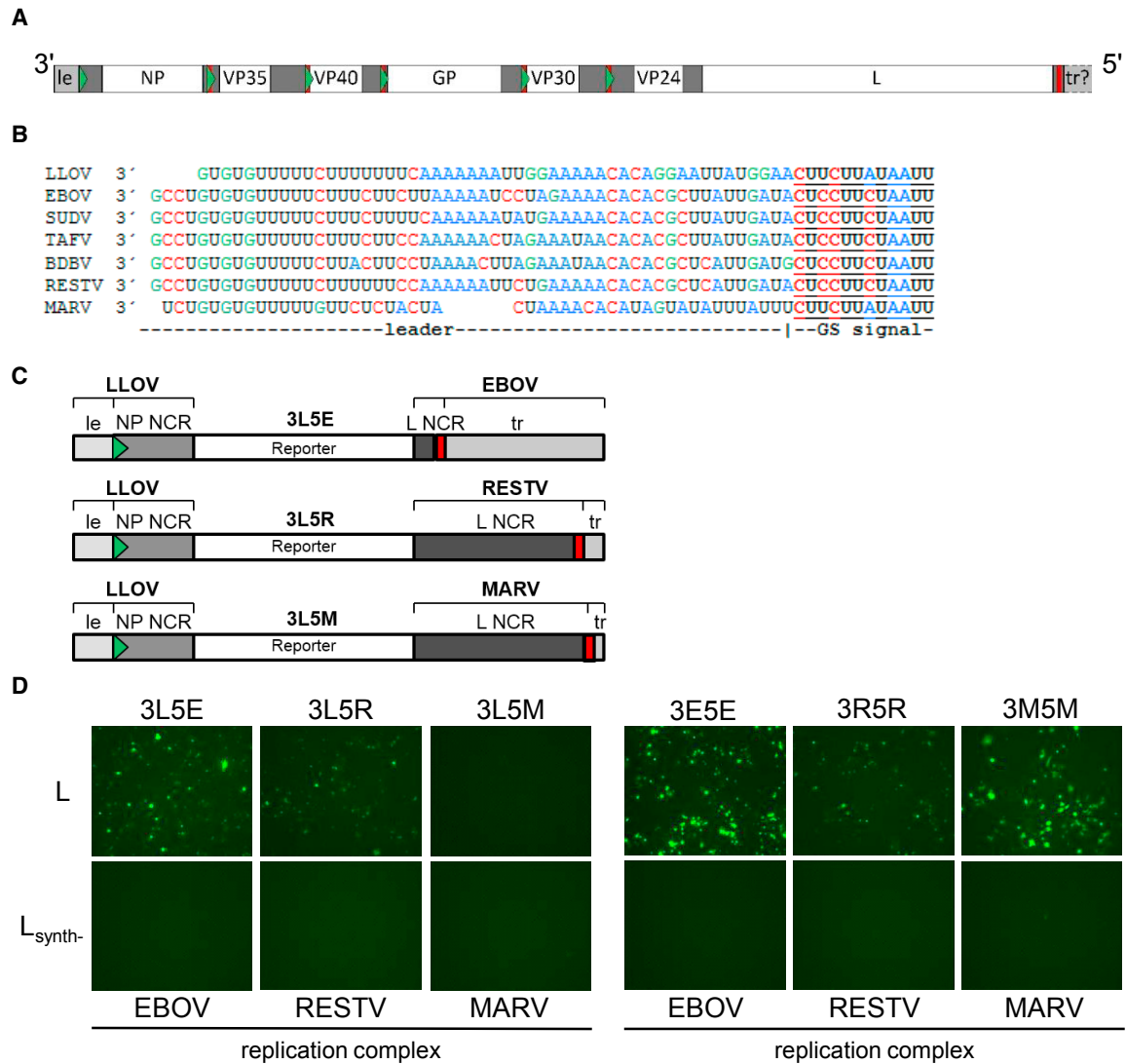


**Figure 1. Chimeric LLOV Minigenomes Are Recognized by the Replication Complexes of Other Filoviruses**

(A) Scheme of the LLOV genome. Solid black lines indicate known sequences, and dotted lines indicate missing sequences. Light gray boxes indicate the leader (le) and trailer (tr). Dark gray boxes indicate non-coding regions flanking the open reading frames (ORFs). ORFs are shown as white boxes. Gene start signals are illustrated as green triangles and gene end signals as red bars.

(B) 3' genome ends of filovirus species. Shown are the sequences of the leaders and NP gene start signals (GS). BDBV, Bundibugyo virus; SUDV, Sudan virus; TAFV, Tai Forest virus.

(C) Schemes of chimeric minigenomes. A reporter gene is flanked by the 3' leader and non-coding region (NCR) of the LLOV NP gene and the 5' NCR of the L gene and trailer of EBOV, RESTV, or MARV.

(D) BSRT7/5 cell were transfected with EGFP-expressing LLOV minigenomes along with the system components of EBOV, RESTV, or MARV, respectively. Authentic filovirus minigenomes were transfected with their corresponding system components as positive controls. L<sub>synth-</sub> indicates the negative control, in which a catalytically inactive L was used. Minigenome activity was visualized 2 DPT. Experiment was performed three times. Representative results are shown.

Unlike other filoviruses, however, it seems that VP24 and L are encoded in a single dicistronic mRNA transcript (Negredo et al., 2011), although this has not been confirmed experimentally.

Transfection studies have shown that LLOV shares many features with other filoviruses. For example, the LLOV GP uses the entry mechanism common to all known filoviruses and, importantly, is able to mediate infection of human cells (Brinkmann et al., 2016; Maruyama et al., 2014; Ng et al., 2014). VP40 in-

duces the formation of filamentous particles and mediates budding (Maruyama et al., 2014), and VP35 acts as an interferon antagonist (Feagins and Basler, 2015). Regarding known differences between MARV and EBOV, LLOV seems to be more closely related to EBOV than MARV. Similar to EBOV, LLOV VP24 is able to block STAT1 nuclear translocation, whereas MARV VP24 lacks this ability. Conversely, unlike MARV VP40, neither EBOV nor LLOV VP40 proteins are able to block

JAK-STAT signaling (Feagins and Basler, 2015). Finally, editing of EBOV and LLOV GP mRNAs is required for the production of the membrane-bound versions of GP, whereas MARV GP does not require mRNA editing to be synthesized (Negredo et al., 2011). Due to the lack of suitable tools, the replication and transcription mechanisms of LLOV have not yet been investigated.

All filoviruses are classified as biosafety level 4 (BSL-4) pathogens, which makes it more difficult to address basic questions about their biology. To overcome this issue, minigenome systems have been widely used to investigate filoviral replication and transcription mechanisms. Minigenomes also provide the basis for developing rescue systems that allow for the generation of infectious virus from cDNA clones (Hoenen et al., 2017). Minigenomes are truncated versions of the viral genomes that contain the *cis*-acting elements required for replication and transcription. These elements are located in the viral genome ends. In a minigenome, the viral genes are typically replaced by a reporter gene. Thus, minigenomes are not infectious and allow for the study of filovirus genome replication and transcription in a low containment setting. An expression plasmid containing the minigenome sequence is used to transfect cells along with plasmids encoding the viral proteins required for viral genome transcription and replication. If the minigenome is accepted as a template by the viral polymerase, the reporter gene is expressed. Minigenome systems are available for EBOV, MARV, and RESTV.

Sequencing of LLOV RNA isolated from dead bats only recovered a partial sequence of the LLOV genome. Compared to the ebola- and marburgvirus genomes, 3 or 4 nucleotides are missing from the 3' end of the LLOV genomic sequence (Figure 1B) and the entire trailer region is missing from the 5' end (Negredo et al., 2011). Because intact 3' and 5' ends are crucial for filovirus replication and transcription, it has not been possible to establish a minigenome system for LLOV. Here, we present the development of a minigenome system in which the missing sequences were complemented by sequences derived from the EBOV, RESTV, or MARV leader and trailer regions. This replication competent system allows for the further study of LLOV replication in cell culture and demonstrates that LLOV is more similar to EBOV and RESTV than MARV regarding its replication and transcription strategies.

## RESULTS

### MARV Replication Complex Does Not Recognize LLOV Leader Sequence as a Template for Transcription

The published LLOV sequence (GenBank: JK828358) lacks the 3' terminal nucleotides and the entire trailer region, and therefore, the virus requires the supplementation of the 3' terminal nucleotides as well as a trailer in order to be replication competent. Sequence comparison to the leader regions of all filovirus species revealed that, intriguingly, LLOV combines conserved *cis*-acting regulatory elements from both ebola- and marburgviruses. Thus, the LLOV leader shows significant homology to ebolavirus sequences, whereas the highly conserved gene start (GS) signal is identical to the MARV GS sequence (Figure 1B). Based on this sequence comparison, we first added the four 3' terminal

ebolavirus nucleotides (3' GCCU) to the LLOV leader region and used the complemented sequence for minigenome construction.

To analyze whether the LLOV leader would be recognized by the EBOV, RESTV, or MARV replication complexes, the complemented LLOV leader region and 3' non-coding region (NCR) (negative sense) of the LLOV NP gene were combined with the EBOV, RESTV, or MARV trailer regions and 5' NCRs (negative sense) of the L genes in EGFP-expressing minigenomes 3L5E, 3L5R, and 3L5M, respectively (Figure 1C). BSR-T7/5 cells were transfected with the chimeric minigenome plasmids along with the corresponding pTM1 system components and visualized for EGFP expression at two days post-transfection (DPTs). As positive controls to ensure that the EBOV, RESTV, and MARV system components were functional, the authentic minigenomes (3E5E, 3R5R, and 3M5M) were used (Figure 1D, right panels). Although EGFP expression was observed in cells transfected with 3L5E and 3L5R and their respective support plasmids, this was not the case in cells transfected with 3L5M and MARV support plasmids (Figure 1D, left panels). MARV-mediated 3L5M minigenome activity was not detected despite multiple attempts with varying plasmid concentrations and culture conditions (data not shown). Of note, the RESTV system components resulted in weaker reporter gene expression with both minigenomes. These data support the previous observation that LLOV might be more closely related to ebolaviruses than to marburgviruses.

### LLOV Replication Complex Recognizes Chimeric LLOV Minigenomes

As a next step toward a LLOV minigenome system, we investigated whether the published LLOV gene sequences encoding the viral proteins required for replication and transcription are expressed into functional proteins. HEK293T cells were transfected with plasmids expressing codon-optimized LLOV NP, VP35, VP30, and L along with the chimeric EGFP or luciferase LLOV minigenomes (3L5E, 3L5R, or 3L5M). Each chimeric LLOV minigenome was accepted as a template for replication and transcription by the LLOV replication complex (Figures 2A and 2B), indicating that the promoter regions within the marburg- and ebolavirus trailers are recognized by the LLOV polymerase. Indeed, these data surprisingly indicate that the LLOV polymerase complex is able to better utilize the L NCR and trailer of MARV than that of EBOV.

Next, we tested whether the authentic EBOV, RESTV, and MARV minigenomes would be accepted as templates by the LLOV polymerase complex. HEK293T cells were transfected with the LLOV system components along with the EBOV, RESTV, or MARV minigenomes. Robust EGFP expression was observed in cells transfected with the LLOV support plasmids and 3E5E and 3R5R, but not 3M5M, indicating that the LLOV replication complex is able to recognize the EBOV and RESTV leader regions, but not the MARV leader, despite the ability of this complex to efficiently utilize the MARV trailer (Figure 2C). These data suggest that the MARV leader sequence might be too divergent from LLOV to be recognized for replication and/or transcription.

Both MARV and EBOV nucleocapsids form large inclusions in the cytoplasm of infected cells that are the sites of viral

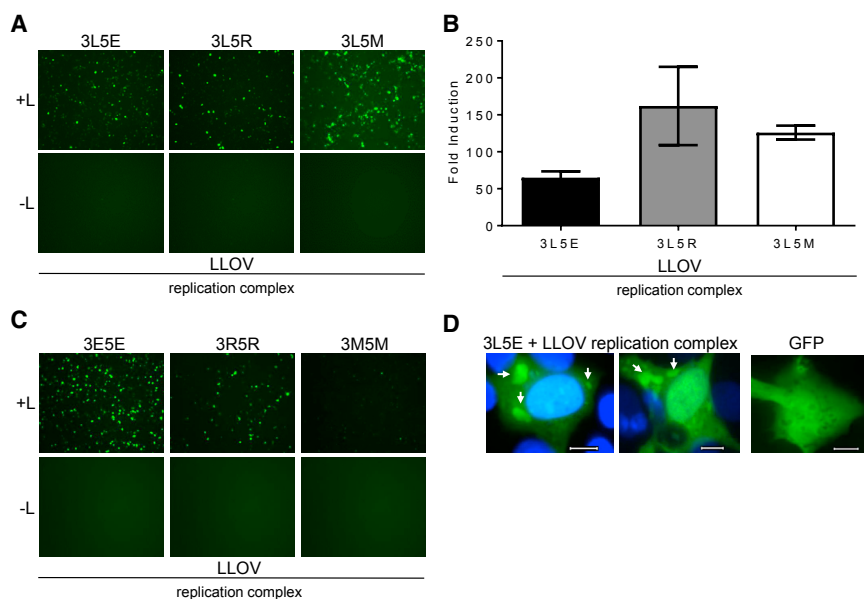


**Figure 2. LLOV Minigenomes Are Accepted as Templates by LLOV Replication Complex**

(A) HEK293T cells were transfected with EGFP-expressing LLOV minigenomes along with LLOV system components. As a negative control, polymerase L was omitted (–L). Minigenome activity was visualized 3 DPT. Experiment was performed three times. Representative results are shown.

(B) HEK293T cells were transfected with firefly luciferase-expressing LLOV minigenomes along with LLOV system components and pMIR β-gal plasmid for normalization. Cells were harvested for analysis 3 DPT. Data represent the means of three independent experiments, and error bars represent ± SEM.

(C) EBOV, RESTV, or MARV EGFP-expressing minigenomes were transfected into HEK293T cells along with LLOV system components. Minigenome activity was visualized 3 DPT. Experiment was performed three times. Representative results are shown.

(D) U2OS cells were transfected with EGFP-expressing minigenome 3L5E along with LLOV system components. Cells were fixed at 3 DPT, and

EGFP expression was visualized by confocal microscopy. Viral inclusions are marked by arrows. Nuclei are stained with DAPI. As a negative control, cells were transfected with pCAGGS-EGFP. Experiment was performed three times. Representative results are shown. Scale bars are 20 μm.

replication (Dolnik et al., 2015; Hoenen et al., 2012). Inclusion formation can be mimicked by transient expression of the nucleocapsid proteins. Unfortunately, there are no antibodies available for the LLOV nucleocapsid proteins to aid in the detection of LLOV inclusions. We have previously shown that various fluorescence proteins, including GFP, colocalize with EBOV and MARV inclusions when co-expressed with the nucleocapsid proteins (Schmidt et al., 2011). To visualize viral inclusions in the LLOV minigenome system, U2OS cells were transfected with minigenome 3L5E-EGFP and LLOV support plasmids for fluorescence microscopy. As a negative control, cells were transfected with a GFP-expressing plasmid. U2OS cells are flat with a large cytoplasm, enabling easy visualization of cytoplasmic structures. Whereas GFP was homogeneously distributed in cells transfected with the GFP expression plasmid in the absence of LLOV system components, GFP accumulated in inclusion-like structures in the cytoplasm of cells transfected with LLOV system components (Figure 2D). These data indicate that the LLOV minigenome system mimics the events that occur during transcription and replication in infected cells.

### LLOV Minigenomes Require VP30 to Support Transcription

Despite many similarities in the replication and transcription strategies of ebola- and marburgviruses, there are also remarkable differences. Although EBOV and RESTV minigenome transcription strongly depends on the presence of the transcription factor VP30 (Boehmann et al., 2005; Mühlberger et al., 1999), this is not the case for the MARV minigenome systems (Albariño et al., 2013; Mühlberger et al., 1998). However, VP30 is required for the rescue of full-length clones of both EBOV and MARV (Albariño et al., 2013; Enterlein et al., 2006; Volchkov et al., 2001). We have previously shown that EBOV

is able to adopt VP30 proteins from other ebolavirus species as well as MARV to retain transcription competency (Boehmann et al., 2005; Mühlberger et al., 1999), and MARV is able to utilize EBOV VP30 for viral rescue (Enterlein et al., 2006). We next sought to investigate whether LLOV minigenome transcription depends on the presence of VP30 and, if this is the case, whether the LLOV transcription complex could utilize VP30 from other filovirus species. Of note, the trailer region is not required for transcriptional activity (Hoenen et al., 2010; Olesen et al., 2018). We transfected cells with 3L5E, 3L5M, and 3L5R minigenomes and LLOV system components, substituting LLOV VP30 for either EBOV, MARV, or RESTV VP30 or an mCherry plasmid to control for the absence of VP30 (Figure 3). Similar to the EBOV and RESTV minigenome systems, transcription of the chimeric LLOV minigenomes was strongly enhanced in the presence of VP30, indicating that LLOV follows an ebolavirus-like transcription strategy (Figure 3). The VP30 proteins of other filoviruses did not efficiently rescue minigenome transcription, although the addition of RESTV VP30 consistently led to more minigenome activity than the addition of EBOV or MARV VP30.

### LLOV Support Plasmids Do Not Accept the MARV 3' Genome Ends as a Template for Transcription

The published LLOV sequence is missing the first nucleotides at the 3' end of the genome, and for our first minigenomes, we included the first 4 nucleotides (3' GCCU) of the ebolavirus species to supplement for the missing sequence (Figure 1B). The LLOV replication complex accepted this leader sequence as a template for transcription and replication in combination with the EBOV, RESTV, and MARV trailers (Figures 2A and 2B). Interestingly, the 3L5M minigenome was accepted by the LLOV, but not MARV, replication complex, and conversely, the 3M5M

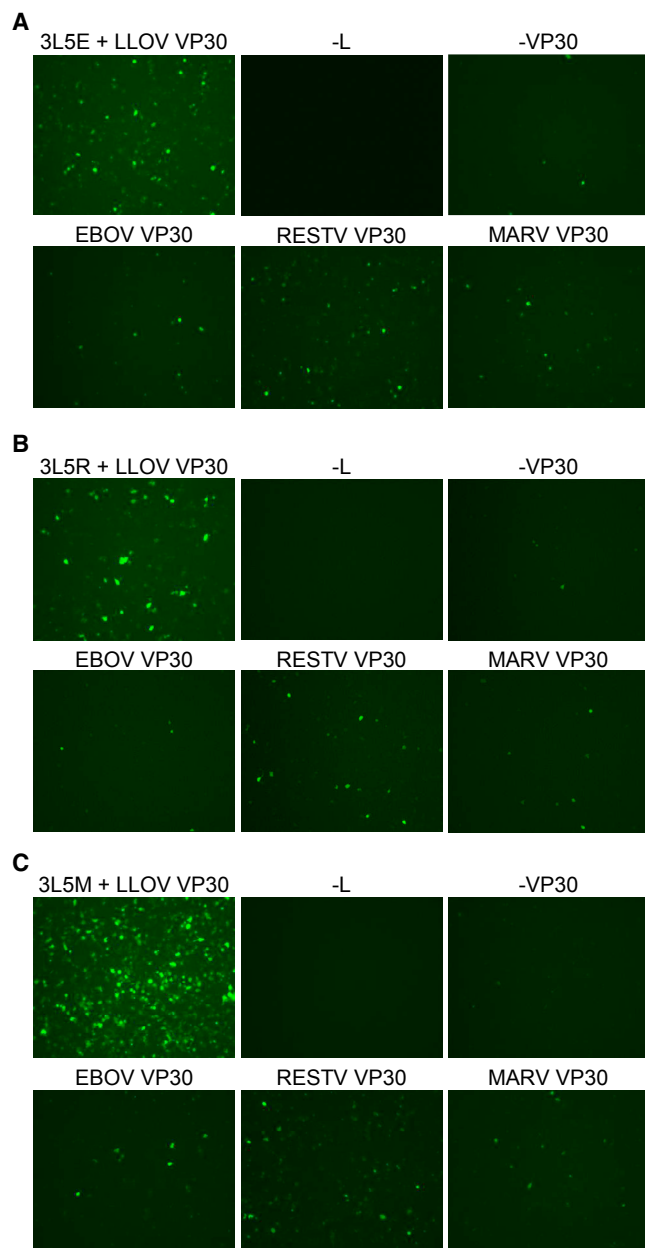


**Figure 3. LLOV Requires VP30 for Transcription**

EGFP-expressing 3L5E (A), 3L5R (B), or 3L5M (C) minigenomes were transfected into HEK293T cells along with LLOV system components, including LLOV VP30. As a negative control, polymerase L was omitted (–L). LLOV VP30 was either omitted (–VP30) or replaced with the VP30 proteins of EBOV, RESTV, or MARV. Minigenome activity was visualized 3 DPT. Experiment was repeated three times, and representative fluorescence images are shown.

minigenome was efficiently replicated by the MARV, but not LLOV, polymerase (Figures 1D and 2A–2C). This suggests that the filoviral leader region contains sequences that provide species specificity. To analyze whether the 3' terminal leader nucleotides determine recognition by the polymerase complex, we generated a 3L5M minigenome that contains the first three nu-

cleotides of the MARV leader (3' UCU; Figure 4A). This minigenome is labeled 3L<sub>M</sub>5M. Cells were transfected with EGFP- or luciferase-expressing minigenome 3L5M or 3L<sub>M</sub>5M along with LLOV system components. Intriguingly, minigenome 3L<sub>M</sub>5M was not recognized as a template for transcription, despite optimizations of the minigenome system and culture conditions (Figures 4B and 4E). To eliminate the possibility that mutations caused this negative result, sequence integrity of the minigenome was confirmed by sequencing, including the hepatitis delta ribozyme and the T7 RNA polymerase promoter regions flanking the minigenome sequence. Because minigenomes 3L5M and 3L<sub>M</sub>5M only differ in the first two or three leader nucleotides, respectively, these data indicate that, indeed, the 3' terminal nucleotides determine promoter recognition by the LLOV polymerase complex. In contrast to LLOV, the MARV polymerase complex was not able to induce reporter gene expression from either minigenome, indicating that, even in the presence of the 3' terminal MARV sequence, the LLOV leader is divergent enough from the MARV leader that it cannot be used as a template for transcription by MARV system components (Figures 4C and 4E).

Previous work on filovirus minigenomes showed that both EBOV and MARV system components were capable of recognizing a chimeric 3E5M minigenome, but neither replication complex could recognize a 3M5E minigenome (Mühlberger et al., 1999). Therefore, we asked the question of whether EBOV system components could recognize minigenomes 3L5M and 3L<sub>M</sub>5M. Cells were transfected with each minigenome and the EBOV system components. Similar to the results with the LLOV system components, the 3L5M, but not 3L<sub>M</sub>5M, minigenome was accepted as a template by the EBOV replication complex, confirming the importance of the 3' terminal nucleotides for promoter recognition (Figures 4D and 4E).

## DISCUSSION

Comparison of genetic sequences of all filoviruses indicates that LLOV evolved from a common ancestor with ebolaviruses after the divergence of marburgviruses (Negredo et al., 2011). Functional analysis of LLOV VP24 and VP35 suggests that LLOV behaves like ebolaviruses (Feagins and Basler, 2015). Our data obtained with the LLOV minigenome system demonstrate that LLOV utilizes a more ebolavirus-like replication strategy, confirming that LLOV is functionally more similar to ebolaviruses than marburgviruses. This is also reflected by the promoter recognition of the LLOV polymerase complex, which requires ebolavirus-like 3' terminal nucleotides for binding. Intriguingly, the first one to two 3' genomic nucleotides seem to determine species specificity of the filoviral polymerases, separating the ebola- and cuevaviruses from the marburgviruses. Conversely and surprisingly, the LLOV polymerase complex seems better able to recognize the 5' end of the MARV genome (NCR of L and trailer) than that of the EBOV genome. Thus, although other data indicate that LLOV in general is more EBOV-like, LLOV appears to have some features that are more MARV-like. In addition to the significant sequence divergence, these data bolster the prior decision to assign LLOV to its own genus, Cuevavirus.

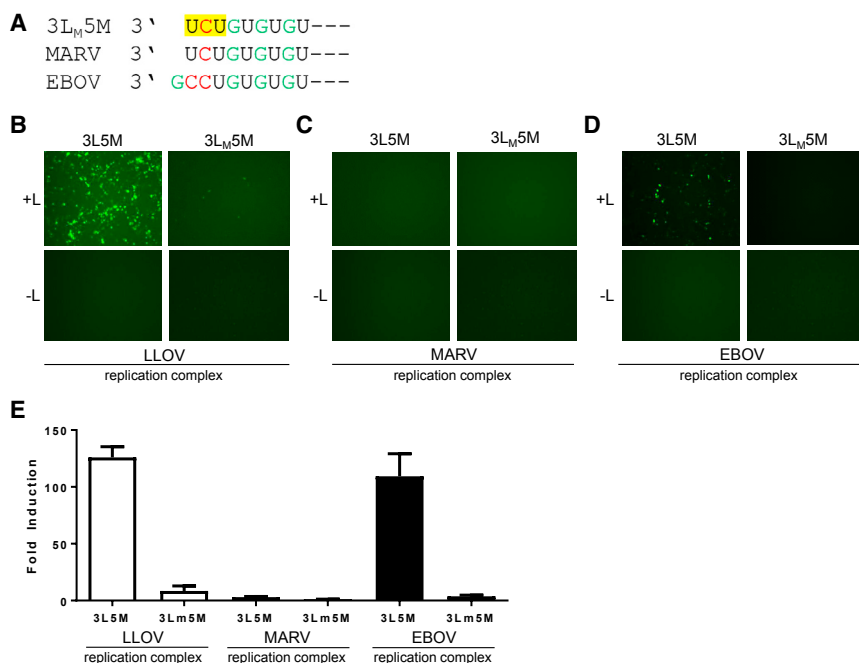


**Figure 4. LLOV Replication Complex Does Not Recognize MARV-like 3' Leader Sequence**

(A) 3' terminal nucleotides of filovirus genomes. The first three nucleotides of the MARV leader sequence (UCU, highlighted) were introduced into the LLOV leader.

(B–D) HEK293T cells were transfected with EGFP-expressing LLOV minigenomes along with LLOV (B), MARV (C), or EBOV (D) system components. As a negative control, polymerase L was omitted (–L). Minigenome activity was visualized 3 DPT. Experiment was repeated three times. Representative images are shown.

(E) HEK293T cells were transfected with firefly luciferase-expressing LLOV minigenomes along with the LLOV system components and pMIR β-gal plasmid for normalization. Cells were harvested for analysis 3 DPT. Data represent the means of three independent experiments, and error bars represent ± SEM.

Minigenome systems have previously been shown to be useful BSL-2 tools for drug discovery against filoviruses (Edwards et al., 2015; Jasenosky et al., 2010; Nelson et al., 2017; Uebelhoer et al., 2014). The LLOV minigenome system described in this study is a valuable addition to this tool kit and could be adapted to a high-throughput format for drug discovery against all filoviruses. However, minigenome systems cannot be used for pathogenesis studies, and the potential for LLOV to cause disease in humans is still unknown. Human cells are permissive to LLOV GP-mediated entry (Maruyama et al., 2014; Ng et al., 2014), and human cells are able to support LLOV replication and transcription, as demonstrated in this study. Antibodies against EBOV and MARV GPs are not cross-reactive against LLOV GP, and therefore, any vaccines currently in development against filoviruses will not be efficacious against LLOV (Maruyama et al., 2014), highlighting the need to study the pathogenic potential of this virus in further detail. Infectious LLOV is indispensable to address these questions. As this is currently not available, rescue of infectious virus from cDNA clones would be a viable alternative. The work presented here informs the generation of infectious LLOV clones, as a functional minigenome system is the first step toward establishing a full-length reverse genetics system for LLOV.

The recent advances in sequencing techniques led to the discovery of a huge number of novel viruses, including filovirus sequences recovered from fish (Shi et al., 2018). As it is the case for LLOV, most of these recently discovered viral sequences lack sequence information, which makes virus rescue challenging. Chimeric viruses that combine the sequences of newly discovered fragmentary viruses with those of closely related viruses are valuable tools for virus rescue (Juozapaitis et al., 2014; Krüger et al., 2016; Zhou et al., 2014). These chimeric

viruses not only enable molecular biology and pathogenesis studies but provide also valuable information about viral evolution.

In conclusion, the LLOV minigenomes presented here allow for the study of LLOV transcription and replication that was previously not possible. This tool can be utilized to rescue infectious LLOV clones and simultaneously be used to further characterize the basic biology of this novel filovirus.

## STAR★METHODS

Detailed methods are provided in the online version of this paper and include the following:

- [KEY RESOURCES TABLE](#)
- [CONTACT FOR REAGENT AND RESOURCE SHARING](#)
- [EXPERIMENTAL MODEL AND SUBJECT DETAILS](#)
  - Cell culture
- [METHOD DETAILS](#)
  - Viral sequences
  - Plasmids
  - Transfection
  - Microscopy
  - Luciferase analysis
- [QUANTIFICATION AND STATISTICAL ANALYSIS](#)
  - Luciferase analysis

## ACKNOWLEDGMENTS

The authors thank U.J. Buchholz, National Institute of Allergy and Infectious Diseases (NIAID)/NIH, Bethesda, MD, for providing BSRT7/5 cells and T. Takimoto, St. Jude Children's Research Hospital, Memphis, TN, and Y. Kawaoka, University of Wisconsin, Madison, WI, for providing the pCAGGS-T7 plasmid. This work was funded by the National Institute of Allergy and Infectious Diseases of the NIH under award numbers R21-AI137793, R21-AI126457, and UC6-AI058618 and by the National Emerging Infectious Diseases Laboratories (NEIDL) Director's Fund.

## AUTHOR CONTRIBUTIONS

W.A.M. and J.R.P. conducted the experiments. W.A.M., J.R.P., A.J.H., T.N.C., and L.R.D. prepared plasmids used in this study. W.A.M., J.R.P., A.J.H., and E.M. designed the experiments. W.A.M., A.J.H., and E.M. wrote the manuscript.

## DECLARATION OF INTERESTS

The authors declare no competing interests.

Received: May 11, 2018

Revised: July 12, 2018

Accepted: August 6, 2018

Published: September 4, 2018

## REFERENCES

- Albariño, C.G., Uebelhoer, L.S., Vincent, J.P., Khristova, M.L., Chakrabarti, A.K., McElroy, A., Nichol, S.T., and Towner, J.S. (2013). Development of a reverse genetics system to generate recombinant Marburg virus derived from a bat isolate. *Virology* 446, 230–237.
- Amarasinghe, G.K., Aréchiga Ceballos, N.G., Banyard, A.C., Basler, C.F., Bavari, S., Bennett, A.J., Blasdel, K.R., Briese, T., Bukreyev, A., Cai, Y., et al. (2018). Taxonomy of the order Mononegavirales: update 2018. *Arch. Virol.* 163, 2283–2294.
- Baize, S., Pannetier, D., Oestereich, L., Rieger, T., Koivogui, L., Magassouba, N., Soropogui, B., Sow, M.S., Keita, S., De Clerck, H., et al. (2014). Emergence of Zaire Ebola virus disease in Guinea. *N. Engl. J. Med.* 371, 1418–1425.
- Bausch, D.G. (2017). West Africa 2013 Ebola: from virus outbreak to humanitarian crisis. *Curr. Top. Microbiol. Immunol.* 411, 63–92.
- Boehmann, Y., Enterlein, S., Randolph, A., and Mühlberger, E. (2005). A reconstituted replication and transcription system for Ebola virus Reston and comparison with Ebola virus Zaire. *Virology* 332, 406–417.
- Brinkmann, C., Nehlmeier, I., Walendy-Gnirß, K., Nehls, J., González Hernández, M., Hoffmann, M., Qiu, X., Takada, A., Schindler, M., and Pöhlmann, S. (2016). The tetherin antagonism of the Ebola virus glycoprotein requires an intact receptor-binding domain and can be blocked by GP1-specific antibodies. *J. Virol.* 90, 11075–11086.
- Buchholz, U.J., Finke, S., and Conzelmann, K.K. (1999). Generation of bovine respiratory syncytial virus (BRSV) from cDNA: BRSV NS2 is not essential for virus replication in tissue culture, and the human RSV leader region acts as a functional BRSV genome promoter. *J. Virol.* 73, 251–259.
- Dolnik, O., Stevermann, L., Kolesnikova, L., and Becker, S. (2015). Marburg virus inclusions: A virus-induced microcompartment and interface to multivesicular bodies and the late endosomal compartment. *Eur. J. Cell Biol.* 94, 323–331.
- Edwards, M.R., Pietzsch, C., Vausselin, T., Shaw, M.L., Bukreyev, A., and Basler, C.F. (2015). High-throughput minigenome system for identifying small-molecule inhibitors of Ebola virus replication. *ACS Infect. Dis.* 1, 380–387.
- Enterlein, S., Volchkov, V., Weik, M., Kolesnikova, L., Volchkova, V., Klenk, H.D., and Mühlberger, E. (2006). Rescue of recombinant Marburg virus from cDNA is dependent on nucleocapsid protein VP30. *J. Virol.* 80, 1038–1043.
- Feagins, A.R., and Basler, C.F. (2015). Lloviu virus VP24 and VP35 proteins function as innate immune antagonists in human and bat cells. *Virology* 485, 145–152.
- Hoenen, T., Jung, S., Herwig, A., Groseth, A., and Becker, S. (2010). Both matrix proteins of Ebola virus contribute to the regulation of viral genome replication and transcription. *Virology* 403, 56–66.
- Hoenen, T., Shabman, R.S., Groseth, A., Herwig, A., Weber, M., Schudt, G., Dolnik, O., Basler, C.F., Becker, S., and Feldmann, H. (2012). Inclusion bodies are a site of ebolavirus replication. *J. Virol.* 86, 11779–11788.
- Hoenen, T., Brandt, J., Cai, Y., Kuhn, J.H., and Finch, C. (2017). Reverse genetics of filoviruses. *Curr. Top. Microbiol. Immunol.* 411, 421–445.
- Jasenosky, L.D., Neumann, G., and Kawaoka, Y. (2010). Minigenome-based reporter system suitable for high-throughput screening of compounds able to inhibit Ebolavirus replication and/or transcription. *Antimicrob. Agents Chemother.* 54, 3007–3010.
- Jones, M.E., Schuh, A.J., Amman, B.R., Sealy, T.K., Zaki, S.R., Nichol, S.T., and Towner, J.S. (2015). Experimental inoculation of Egyptian Rousette bats (*Rousettus aegyptiacus*) with viruses of the ebolavirus and marburgvirus genera. *Viruses* 7, 3420–3442.
- Juozapaitis, M., Aguiar Moreira, É., Mena, I., Giese, S., Riegger, D., Pohlmann, A., Höper, D., Zimmer, G., Beer, M., García-Sastre, A., and Schwemmler, M. (2014). An infectious bat-derived chimeric influenza virus harbouring the entry machinery of an influenza A virus. *Nat. Commun.* 5, 4448.
- Kemenesi, G., Kurucz, K., Dallos, B., Zana, B., Földes, F., Boldogh, S., Görfö, T., Carroll, M.W., and Jakab, F. (2018). Re-emergence of Lloviu virus in *Miniopterus schreibersii* bats, Hungary, 2016. *Emerg. Microbes Infect.* 7, 66.
- Krüger, N., Sauder, C., Hoffmann, M., Örvell, C., Drexler, J.F., Rubin, S., and Herrler, G. (2016). Recombinant mumps viruses expressing the batMuV fusion glycoprotein are highly fusion active and neurovirulent. *J. Gen. Virol.* 97, 2837–2848.
- Marí Saéz, A., Weiss, S., Nowak, K., Lapeyre, V., Zimmermann, F., Düx, A., Kühl, H.S., Kaba, M., Regnaut, S., Merkel, K., et al. (2015). Investigating the zoonotic origin of the West African Ebola epidemic. *EMBO Mol. Med.* 7, 17–23.
- Maruyama, J., Miyamoto, H., Kajihara, M., Ogawa, H., Maeda, K., Sakoda, Y., Yoshida, R., and Takada, A. (2014). Characterization of the envelope glycoprotein of a novel filovirus, lloviu virus. *J. Virol.* 88, 99–109.
- Miranda, M.E., and Miranda, N.L. (2011). Reston ebolavirus in humans and animals in the Philippines: a review. *J. Infect. Dis.* 204 (Suppl 3), S757–S760.
- Mühlberger, E., Löffering, B., Klenk, H.-D., and Becker, S. (1998). Three of the four nucleocapsid proteins of Marburg virus, NP, VP35, and L, are sufficient to mediate replication and transcription of Marburg virus-specific monocistronic minigenomes. *J. Virol.* 72, 8756–8764.
- Mühlberger, E., Weik, M., Volchkov, V.E., Klenk, H.-D., and Becker, S. (1999). Comparison of the transcription and replication strategies of marburg virus and Ebola virus by using artificial replication systems. *J. Virol.* 73, 2333–2342.
- Negredo, A., Palacios, G., Vázquez-Morón, S., González, F., Dopazo, H., Moler, F., Juste, J., Quetglas, J., Savji, N., de la Cruz Martínez, M., et al. (2011). Discovery of an ebolavirus-like filovirus in Europe. *PLoS Pathog.* 7, e1002304.
- Nelson, E.V., Pacheco, J.R., Hume, A.J., Cressey, T.N., Deflubé, L.R., Ruedas, J.B., Connor, J.H., Ebihara, H., and Mühlberger, E. (2017). An RNA polymerase II-driven Ebola virus minigenome system as an advanced tool for antiviral drug screening. *Antiviral Res.* 146, 21–27.
- Ng, M., Ndungo, E., Jangra, R.K., Cai, Y., Postnikova, E., Radoshitzky, S.R., Dye, J.M., Ramírez de Arellano, E., Negredo, A., Palacios, G., et al. (2014). Cell entry by a novel European filovirus requires host endosomal cysteine proteases and Niemann-Pick C1. *Virology* 468–470, 637–646.
- Olsen, M.E., Cressey, T.N., Mühlberger, E., and Connor, J.H. (2018). Differential mechanisms for the involvement of polyamines and hypusine eIF5A in Ebola virus gene expression. *J. Virol.* Published online July 25, 2018. <https://doi.org/10.1128/JVI.01260-18>.
- Paweska, J.T., Storm, N., Grobbelaar, A.A., Markotter, W., Kemp, A., and Jansen van Vuren, P. (2016). Experimental inoculation of Egyptian fruit bats (*Rousettus aegyptiacus*) with Ebola virus. *Viruses* 8, E29.
- Schmidt, K.M., Schumann, M., Olejnik, J., Krähling, V., and Mühlberger, E. (2011). Recombinant Marburg virus expressing EGFP allows rapid screening of virus growth and real-time visualization of virus spread. *J. Infect. Dis.* 204 (Suppl 3), S861–S870.
- Shi, M., Lin, X.D., Chen, X., Tian, J.H., Chen, L.J., Li, K., Wang, W., Eden, J.S., Shen, J.J., Liu, L., et al. (2018). The evolutionary history of vertebrate RNA viruses. *Nature* 556, 197–202.
- Towner, J.S., Amman, B.R., Sealy, T.K., Carroll, S.A., Comer, J.A., Kemp, A., Swanepoel, R., Paddock, C.D., Balinandi, S., Khristova, M.L., et al. (2009). Isolation of genetically diverse Marburg viruses from Egyptian fruit bats. *PLoS Pathog.* 5, e1000536.

Uebelhoer, L.S., Albariño, C.G., McMullan, L.K., Chakrabarti, A.K., Vincent, J.P., Nichol, S.T., and Towner, J.S. (2014). High-throughput, luciferase-based reverse genetics systems for identifying inhibitors of Marburg and Ebola viruses. *Antiviral Res.* *106*, 86–94.

Volchkov, V.E., Volchkova, V.A., Mühlberger, E., Kolesnikova, L.V., Weik, M., Dolnik, O., and Klenk, H.D. (2001). Recovery of infectious Ebola virus from

complementary DNA: RNA editing of the GP gene and viral cytotoxicity. *Science* *291*, 1965–1969.

Zhou, B., Ma, J., Liu, Q., Bawa, B., Wang, W., Shabman, R.S., Duff, M., Lee, J., Lang, Y., Cao, N., et al. (2014). Characterization of uncultivable bat influenza virus using a replicative synthetic virus. *PLoS Pathog.* *10*, e1004420.

## STAR★METHODS

### KEY RESOURCES TABLE

REAGENT or RESOURCE	SOURCE	IDENTIFIER
Chemicals, Peptides, and Recombinant Proteins		
Transfection reagent: Lipofectamine LTX	Life Technologies	Cat#15338100
Transfection reagent: Trans-IT LT1	Mirus Bio	Cat#MIR 2304
Restriction enzyme: NdeI	New England Biolabs	Cat#R0111S
Restriction enzyme: NotI	New England Biolabs	Cat#R0189S
Restriction enzyme: RsrII	New England Biolabs	Cat#R0501S
DNA Polymerase: PfuUltra Hotstart DNA Polymerase	Agilent Technologies	Cat#600390
Critical Commercial Assays		
Luciferase Assay System	Promega	Cat#E1500
β-Galactosidase Enzyme Assay System with Reporter Lysis Buffer	Promega	Cat#E2000
Experimental Models: Cell Lines		
Human embryonic kidney cell line HEK293T	ATCC	CRL-3216
Human osteosarcoma cell line U2OS	ATCC	HTB-96
Golden hamster cell line Bsr-T7/5	U. J. Buchholz, NIAID/NIH, Bethesda, MD, USA	( <a href="#">Buchholz et al., 1999</a> )
Oligonucleotides		
Primer: eGFP-NdeI fwd: GTC CAT ATG ATG GTG AGC AAG GGC GAG GAG CTG TTC ACC	This paper	N/A
Primer: eGFP-NotI rev: GAT GCG GCC GCT TAC TTG TAC AGC TCG TCC ATG CC	This paper	N/A
Recombinant DNA		
Plasmid: pCAGGS-LLOV NP	This paper	N/A
Plasmid: pCAGGS-LLOV VP35	This paper	N/A
Plasmid: pCAGGS-LLOV VP30	This paper	N/A
Plasmid: pCAGGS-LLOV L	This paper	N/A
Plasmid: pTM1-EBOV NP	Mühlberger lab	Addgene Plasmid #69121
Plasmid: pTM1-EBOV VP35	Mühlberger lab	Addgene Plasmid #68121
Plasmid: pTM1-EBOV VP30	Mühlberger lab	Addgene Plasmid #69119
Plasmid: pTM1-EBOV L	Mühlberger lab	Addgene Plasmid #69120
Plasmid: pTM1-EBOV L <sub>synth</sub>	Mühlberger lab	This paper
Plasmid: pCAGGS-EBOV NP	Mühlberger lab	Addgene Plasmid #103049
Plasmid: pCAGGS-EBOV VP35	Mühlberger lab	Addgene Plasmid #103050
Plasmid: pCAGGS-EBOV VP30	Mühlberger lab	Addgene Plasmid #103051
Plasmid: pCAGGS-EBOV L	Mühlberger lab	Addgene Plasmid #103052
Plasmid: pTM1-RESTV NP	Mühlberger lab	<a href="#">Boehmann et al., 2005</a>
Plasmid: pTM1-RESTV VP35	Mühlberger lab	<a href="#">Boehmann et al., 2005</a>
Plasmid: pTM1-RESTV VP30	Mühlberger lab	<a href="#">Boehmann et al., 2005</a>
Plasmid: pTM1-RESTV L	Mühlberger lab	<a href="#">Boehmann et al., 2005</a>
Plasmid: pTM1-RESTV L <sub>synth</sub>	Mühlberger lab	This paper
Plasmid: pCAGGS-RESTV VP30	Mühlberger lab	This paper
Plasmid: pTM1-MARV NP	Mühlberger lab	<a href="#">Mühlberger et al., 1998</a>
Plasmid: pTM1-MARV VP35	Mühlberger lab	<a href="#">Mühlberger et al., 1998</a>
Plasmid: pTM1-MARV VP30	Mühlberger lab	<a href="#">Mühlberger et al., 1998</a>
Plasmid: pTM1-MARV L	Mühlberger lab	<a href="#">Mühlberger et al., 1998</a>

(Continued on next page)

**Continued**

REAGENT or RESOURCE	SOURCE	IDENTIFIER
Plasmid: pTM1-MARV <sub>L<sub>synth</sub></sub>	Mühlberger lab	This paper
Plasmid: pCAGGS-MARV NP	Mühlberger lab	This paper
Plasmid: pCAGGS-MARV VP35	Mühlberger lab	This paper
Plasmid: pCAGGS-MARV VP30	Mühlberger lab	This paper
Plasmid: pCAGGS-MARV L	Mühlberger lab	This paper
Plasmid: p2,0-3E5E-EGFP	Mühlberger lab	Addgene Plasmid #69359
Plasmid: p2,0-3R5R-EGFP	Mühlberger lab	This paper
Plasmid: p2,0-3M5M-EGFP	Mühlberger lab	This paper
Plasmid: p2,0-3L5E-EGFP	Mühlberger lab	This paper
Plasmid: p2,0-3L5R-EGFP	Mühlberger lab	This paper
Plasmid: p2,0-3L5M-EGFP	Mühlberger lab	This paper
Plasmid: p2,0-3L5E-Luc	Mühlberger lab	This paper
Plasmid: p2,0-3L5R-Luc	Mühlberger lab	This paper
Plasmid: p2,0-3L5M-Luc	Mühlberger lab	This paper
Plasmid: p2,0-3L <sub>M</sub> 5M-EGFP	Mühlberger lab	This paper
Plasmid: p2,0-3L <sub>M</sub> 5M-Luc	Mühlberger lab	This paper
Plasmid: pMIR β-gal	M. Jones, Boston University, Boston, MA, Invitrogen	Catalog # AM5795
Plasmid: pCDNA3.1-mCherry	V. von Messling, Paul Ehrlich Institute, Langen, Germany	N/A
Plasmid: pCAGGS-GFP	Mühlberger lab	<a href="#">Schmidt et al., 2011</a>
Plasmid: pCAGGS-T7	T. Takimoto, St. Jude Children's Research Hospital, Memphis, TN, USA and Y. Kawaoka, University of Wisconsin, Madison, WI, USA	N/A
Plasmid: p2,0-3M5M-CAT	Mühlberger lab	<a href="#">Mühlberger et al., 1998</a>
Plasmid: p2,0-3R5R-CAT	Mühlberger lab	<a href="#">Boehmann et al., 2005</a>
Software and Algorithms		
GraphPad Prism 5	GraphPad	N/A
Zeiss Zen version 2.3	Zeiss	N/A
ImageJ version 1.52d	NIH	<a href="https://imagej.nih.gov/ij/">https://imagej.nih.gov/ij/</a>

**CONTACT FOR REAGENT AND RESOURCE SHARING**

Further information and requests for resources and reagents should be directed to and will be fulfilled by the Lead Contact, Elke Mühlberger ([muehlber@bu.edu](mailto:muehlber@bu.edu)).

**EXPERIMENTAL MODEL AND SUBJECT DETAILS**

**Cell culture**

Cell lines used in this study include human embryonic kidney cells (HEK293T; ATCC CRL-3216), human epithelial osteosarcoma epithelial cells (U2OS; ATCC HTB-96), and the hamster baby kidney cell line BSR-T7/5 constitutively expressing T7 RNA polymerase ([Buchholz et al., 1999](#)). HEK293T and U2OS cells were maintained in Dulbecco's modified Eagle medium (DMEM) supplemented with 10% fetal bovine serum (FBS), penicillin (50 units/ml), streptomycin (50 mg/ml) and L-glutamine (200 mM). The BSR-T7/5 cells were maintained in Glasgow's Minimum Essential Medium (G-MEM) supplemented with 10% FBS, L-glutamine (200 mM), 2% MEM amino acid solution (50x) and 10% FBS, with geneticin antibiotic selection (1 mg/ml). All cell lines were grown at 37°C. HEK293T and U2OS are female human cell lines and BSR-T7/5 is a male golden hamster cell line.

## METHOD DETAILS

### Viral sequences

The following NCBI reference filovirus sequences were used for cloning where indicated and for sequence comparison: Lloviu cuevavirus isolate Lloviu virus/M.schreibersii-wt/ESP/2003/Asturias-Bat86 (GenBank: NC\_016144), Zaire ebolavirus isolate Ebola virus/H.sapiens-tc/COD/1976/Yambuku-Mayinga (NC\_002549), Sudan ebolavirus isolate Sudan virus/H.sapiens-tc/UGA/2000/Gulu-808892 (NC\_006432), Tai Forest ebolavirus isolate Tai Forest virus/H.sapiens-tc/CIV/1994/Pauleoula-CI (NC\_014372), Bundibugyo ebolavirus isolate Bundibugyo virus/H.sapiens-tc/UGA/2007/Butalya-811250 (NC\_014373), Reston ebolavirus isolate Reston virus/M.fascicularis-tc/USA/1989/Philippines89-Pennsylvania (NC\_004161), and Marburg marburgvirus isolate Marburg virus/H.sapiens-tc/KEN/1980/Mt. Elgon-Musoke (NC\_001608).

### Plasmids

LLOV NP, VP35, VP30, and L sequences (GenBank: JF828358.1) were codon-optimized for humans, synthesized and cloned into a pCAGGS background (GeneArt/ThermoFisher Scientific). EBOV, MARV, or RESTV NP, VP35, VP30, and L genes were cloned in pTM1 and pCAGGS expression vectors ([https://www.addgene.org/Elke\\_Muhlberger/](https://www.addgene.org/Elke_Muhlberger/)) (Boehmann et al., 2005; Mühlberger et al., 1998). Similar to a previously described replication-deficient EBOV L mutant in pCAGGS (Nelson et al., 2017), replication-deficient EBOV, MARV, and RESTV L mutants ( $L_{\text{synth-}}$ ) were generated by *in vitro* mutagenesis using the respective wild-type pTM1 L plasmids as templates, the corresponding forward and reverse  $L_{\text{synth-}}$  primers, and the Q5 Site Directed Mutagenesis Kit (New England Biolabs) (see [Key Resources Table](#)). These mutants contain an N to A substitution within the highly conserved GDNQ motif at the catalytic site. In the MARV  $L_{\text{synth-}}$ , it is an N<sub>746</sub> to A substitution. In the RESTV  $L_{\text{synth-}}$ , it is an N<sub>743</sub> to A substitution. To create a 3M5M-EGFP minigenome, the EGFP gene was amplified by PCR using pCAGGS-EGFP as a template, primers eGFP-NdeI fwd and eGFP-NotI rev, and PfuUltra HotStart (Agilent Technologies). The PCR fragment was then cloned into the 3M5M-CAT minigenome, replacing the CAT gene, using NdeI and NotI restriction enzymes. A 3R5R-EGFP minigenome was created by replacing the CAT gene of the 3R5R-CAT minigenome with the EGFP gene from the 3M5M-EGFP minigenome via NdeI and NotI. The missing 3' terminal nucleotides of the LLOV leader sequence (GenBank: JF828358.1) were complemented based on sequence comparison with marburg- and ebolavirus genomes (Figure 1B). The EBOV-like 3' terminal nucleotides are GCCU, and the MARV-like 3' terminal nucleotides are UCU. The LLOV leader sequence containing EBOV-like 3' ends was synthesized (GeneArt/ThermoFisher Scientific) and combined with the EBOV trailer from minigenome 3E5E (Mühlberger et al., 1999), the MARV trailer from minigenome 3M5M (Mühlberger et al., 1998), or the RESTV trailer from minigenome 3R5R (Boehmann et al., 2005). The original leader regions of these minigenomes were replaced with the synthesized LLOV leader using NdeI and RsrII restriction sites. This resulted in minigenomes 3L5E, 3L5M, and 3L5R respectively (EGFP and Luc versions each). The 3L<sub>M</sub>5M-Luc and 3L<sub>M</sub>5M-EGFP minigenomes were created by *in vitro* mutagenesis using the 3L5M-Luc and 3L5M-EGFP vectors, respectively, as templates, the MARV-like leader fwd and rev primers, and the Q5 Site Directed Mutagenesis Kit (New England Biolabs) (see [Key Resources Table](#)). All minigenomes are under the control of the T7 RNA polymerase promoter.

### Transfection

$4 \times 10^5$  BSR-T7/5 cells per well were seeded in a 6-well plate one day prior to transfection.  $2 \times 10^5$  HEK293T or U2OS cells per well were seeded in a 12-well plate one day prior to transfection. The next day, cells were transfected with minigenome plasmid DNA along with EBOV, LLOV, MARV, or RESTV support plasmids encoding NP, VP35, VP30, and L. BSR-T7/5 cells were transfected with pTM1 support plasmids, and 293T and U2OS cells were transfected with pCAGGS plasmids. As negative controls for pTM1 EBOV, RESTV, and MARV minigenome systems, L was replaced with replication-deficient L mutants ( $L_{\text{synth-}}$ ). As negative controls for pCAGGS minigenome systems, pCDNA3.1-mCherry plasmid was used instead of L plasmids. pCDNA3.1-mCherry was used instead of VP30 when VP30 was omitted. In the case of 293T cells, plasmid pC-T7/Pol expressing the T7 RNA polymerase was also transfected. When luciferase-expressing minigenomes were used, plasmid pMIR  $\beta$ -gal expressing  $\beta$ -galactosidase, was co-expressed to normalize against transfection efficiency.

Transfection of BSR-T7/5 cells was performed using Lipofectamine LTX with Plus reagent (Life Technologies). Plasmid DNA amounts are indicated below. EGFP minigenome activity was visualized at 2 days post transfection.

Transfection of HEK293T and U2OS cells was performed using Trans-IT LT1 (Mirus Bio). Plasmid DNA amounts are indicated below. Depending on the reporter gene encoded by the minigenome, the cells were used to visualize EGFP expression or lysed to determine luciferase activity at 3 days post transfection (see [Luciferase Analysis](#) for more detail).

For the EBOV pTM1 plasmids, the following amounts of DNA were added to each transfection mix: 1.5  $\mu$ g of minigenome, 100 ng of L or  $L_{\text{synth-}}$ , 500 ng of NP, 500 ng of VP35, and 100 ng of VP30. For the MARV pTM1 plasmids, the following amounts of DNA were added to each transfection mix: 1.5  $\mu$ g of minigenome, 1  $\mu$ g of L or  $L_{\text{synth-}}$ , 500 ng of NP, 500 ng of VP35, and 100 ng of VP30. For the RESTV pTM1 plasmids, the following amounts of DNA were added to each transfection mix: 1.5  $\mu$ g of minigenome, 1  $\mu$ g of L or  $L_{\text{synth-}}$ , 500 ng of NP, 500 ng of VP35, and 500 ng of VP30. For the LLOV pCAGGS plasmids, the following amounts of DNA were added to each transfection mix: 750 ng of minigenome, 100 ng of LLOV L or pCDNA3.1 mCherry, 500 ng of LLOV NP, 125 ng of LLOV VP35, 50 ng of filovirus VP30 or pCDNA3.1 mCherry, and 500 ng of T7 RNA polymerase. For the MARV pCAGGS plasmids, the following amounts of DNA were added to each transfection mix: 750 ng of minigenome, 1  $\mu$ g of L or pCDNA3.1 mCherry, 200 ng of NP, 50 ng of

VP35, 50 ng of VP30, and 500 ng of T7 RNA polymerase. For the EBOV pCAGGS plasmids, the following amounts of DNA were added to each transfection mix: 750 ng of minigenome, 100 ng of L or pCDNA3.1 mCherry, 250 ng of NP, 250 ng of VP35, 50 ng of VP30, and 500 ng of T7 RNA polymerase.

### Microscopy

$2 \times 10^5$  U2OS cells per well were seeded on coverslips in a 12-well plate one day prior to transfection. The next day, cells were transfected with pCAGGS LLOV support plasmids encoding NP, VP35, VP30, and L and the 3L5E EGFP-expressing minigenome as described above. As a transfection control, a pCAGGS-GFP plasmid was transfected alone. At 3 days post transfection, cells were fixed using 1 ml of 4% PFA in DMEM for 15 minutes at room temperature and stained with 2  $\mu$ g of DAPI in 25  $\mu$ l of PBS for 1 hour at room temperature. Imaging was performed using a Zeiss confocal microscope. Image acquisition and processing software used includes the Zeiss software Zen and ImageJ.

### Luciferase analysis

Transfected 293T cells seeded in 12-well plates were harvested using 350  $\mu$ l of Reaction Lysis Buffer from the Luciferase Assay System (Promega) per well. Cell lysates were diluted 1:100 in 1X Reaction Lysis Buffer (Promega). 50  $\mu$ l of diluted lysates were mixed with 50  $\mu$ l of Firefly Luciferase Reagent, and luciferase activity was measured on a BMG Labtech Omega luminometer. To account for potential differences in transfection efficiency, luciferase values were normalized to  $\beta$ -galactosidase values. 50  $\mu$ l of undiluted cell lysates were mixed with 50  $\mu$ l of 2x Assay Buffer (Promega) and incubated for 30 minutes at 37°C. Reaction was terminated by adding 150  $\mu$ l of 1 M sodium carbonate (Promega).  $\beta$ -galactosidase values were measured on a Tecan Spark microplate reader at 420 nm and normalized to a standard curve generated with the  $\beta$ -galactosidase provided by Promega.

## QUANTIFICATION AND STATISTICAL ANALYSIS

### Luciferase analysis

Luciferase values, reported in Figures 2B and 4E, were calculated as fold induction over the values of the negative controls, as determined by value of the Firefly Luc Assay System divided by the  $\beta$ -gal value (see [Methods Details](#)). Standard error of the mean (SEM) and two-tailed t tests for these figures were calculated using GraphPad Prism software.